Materials Science & Engineering A 683 (2017) 110–115

Contents lists available at ScienceDirect

Materials Science & Engineering A

journal homepage: www.elsevier.com/locate/msea

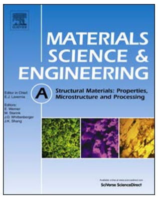

# Strengthening 42CrMo4 steel by isothermal transformation below martensite start temperature

Jian Feng, Timo Frankenbach, Marc Wettlaufer*

*Centre of Materials Engineering, Heilbronn University, Max-Planck-Str. 39, 74081 Heilbronn, Germany*

## ARTICLE INFO

*Keywords:*
Strength and ductility
Austempering
Lower bainite
Fracture
Ultrafine-grained
Nanostructured

## ABSTRACT

Ultrahigh-strength low alloy 42CrMo4 steels, widely used in the automobile industry, were heat treated by two different cycles, namely: conventional austempering above the martensite start temperature $M_S$ and low-temperature isothermal transformation below $M_S$, 604 K (331 °C). Metallurgical and mechanical properties of the heat-treated alloys were investigated carefully by various analysation techniques. The results of tensile testing indicated that the proof strength and ultimate tensile strength could be significantly improved by isothermal transformation below $M_S$ at 583 K (310 °C) for 3.6 ks without degrading the ductility. The ultrafine-grained/nanostructured mixed lower bainite/martensite microstructure created by quenching and partitioning martensite, and the unique fracture morphology were found to be responsible for this improvement. To further confirm the experimental results, a micromechanical model was employed to analyse the strengthening mechanisms.

## 1. Introduction

The mechanical behaviour of complex mixed microstructures in ultrahigh-strength low alloy (USLA) steels has been extensively investigated for many years [1–3]. Generally, there are two conceivable processing routes to attain a mixed bainite and martensite (B/M) microstructure. The first route is bainite formation followed by martensite formation. The process begins with full austenitisation, followed by an isothermal transformation in the bainite range and ends by quenching with or without further tempering (i.e. conventional austempering followed by quenching). The ratio of B/M is determined by the soaking time at the bainite range. A longer duration results in a more complete bainitic transformation thus a larger amount of bainite and simultaneously less untransformed austenite. Quenching after the isothermal transformation yields the formation of martensite from the untransformed austenite.

The impact of bainite on the mechanical properties of B/M USLA steels, created by the first route, has been investigated systematically. Tomita et al. [4–6] suggested that the mechanical properties of USLA steels having a mixed structure of B/M were dominated by the size, shape, and distribution of bainite within martensite. Daigne et al. [7] described the relationship between the yield stress and the B/M microstructural parameters. Young and Bhadeshia [8] modelled the mechanical properties of B/M in their tempered states and revealed that the strength of the bainite could be enhanced via plastic constraint by the surrounding stronger martensite.

The second route is martensite formation followed by bainite formation. Unlike quenching and tempering or conventional austempering, Edmonds et al. [9] claimed in 2006 that martensite could be treated by combining quenching below $M_s$ but still above the martensite-finish temperature $M_f$ and directly tempering either at or above the initial quench temperature $T_Q$. Typically, the partitioning of carbon from martensite to austenite takes place at intermediate temperatures, at which the formation of bainite is favoured [10]. However, to the authors' knowledge, such a concept, i.e. quenching and partitioning martensite [11] or isothermal transformation below $M_s$, has not been successfully applied on steels other than high-Si super bainite. Ideally, in the case of USLA steels without sufficient Si and/or Al, which can effectively suppress carbide formation during partitioning, the carbon-rich austenite is unstable during partitioning and prefers to transform to bainite. In this case, the ratio of B/M is controlled primarily by $T_Q$ and subsequently by the duration of partitioning. Deeper $T_Q$ leads to a high amount of martensite, a smaller portion of untransformed austenite and eventually less bainite. A shorter duration of partitioning retains more untransformed austenite, resulting in more martensite and less bainite after the final quench.

The objective of this study is to design more attractive steels with ultra-fine grained and nanostructured (UFG/NS) mixed B/M microstructure via the second route. However, such an objective is quite challenging due to two factors: (i) metastable B/M microstructures (at

---

* Corresponding author.
*E-mail address:* marc.wettlaufer@hs-heilbronn.de (M. Wettlaufer).

http://dx.doi.org/10.1016/j.msea.2016.12.013
Received 9 August 2016; Received in revised form 1 December 2016; Accepted 2 December 2016

**Table 1**
Chemical compositions (in wt%), martensite start temperature $M_s$ (in K) determined by DSC and theoretical calculations, and martensite finish temperature $M_f$ (in K) determined by DSC and confirmed by [15] of 42CrMo4 steel studied.

| C | Si | Mn | S | P | Cr | Mo | Fe | $M_s$ | $M_f$ |
|---|---|---|---|---|---|---|---|---|---|
| 0.40 | 0.35 | 0.82 | 0.018 | 0.007 | 0.90 | 0.11 | Bal. | 604 | 383 |

room temperature) are usually difficult to create accurately due to the various and complex morphology of bainite, which can only be roughly defined by the transformation temperature [12,13]; (ii) the thermodynamic and kinetic characteristics of phase transformations are difficult to formulate. Heterogeneous phase transformations can be accelerated or inhibited due to interactions between metastable phases, as well as the local para-equilibrium status induced by carbon partitioning and redistribution [14]. To provide the experimental basis for further thermodynamic and kinetic modelling, the present study uses a one-step isothermal transformation below $M_s$ to create a mixed microstructure containing UFG/NS acicular LB/M, aiming to investigate the correlation between the microstructure and mechanical properties in USLA 42CrMo4 steels.

## 2. Experimental procedures

Versatile 42CrMo4 (DIN 1.7225, AISI 4140) steel was used in the present investigation. The chemical composition of the alloy is represented in Table 1, determined by glow discharge optical emission spectroscopy (GD-OES). In order to obtain a range of mixed bainite/martensite (B/M) microstructures, samples were conventionally austempered above $M_s$, at 623 K (350 °C) and alternatively, low-temperature isothermal transformed below $M_s$, at 583 K (310 °C). The detailed heat treatment cycles are listed in Table 2. After isothermal transformation, specimens were quenched and machined for tensile testing, which was performed at room temperature. The size and geometry of the specimens as well as the testing procedure were in accordance with specifications of DIN 50125. The B/M morphology and microstructure were characterized by reflected optical microscopy (OM) and transmission electron microscopy (TEM), subsequently verified by microhardness testing. The phase fraction was analysed graphically under OM. The ductility was determined by the contraction and strain at fracture. Additionally, fracture surfaces of tensile specimens were analysed by scanning electron microscopy (SEM) to determine the fracture mode.

## 3. Results

### 3.1. Morphology and microstructure

The conventional austempering was performed at 623 K (350 °C), and the general effect of varying the austempering duration is shown in Fig. 1a-f. Tint etching indicates that the fraction of bainite (in dark-blue) increases from 40 vol% to 65 vol% while that of martensite (in dark-yellow/brown) decreases. After Nital-etching, upper and lower bainite can easily be distinguished using routine microscopy. The upper bainite (UB), which usually is coherent with the prior austenite matrix, consists of tiny cementite strings that are generally oriented parallel to the long direction of the ferrite needles, partly occupying the prior austenite grain. Acicular LB partitions distinguishably in prior austenite grains, classically demonstrated in Fig. 1g-j (partly in Fig. 1a-f as well). The size and spacing of the carbide platelets/strings in UB and LB, which varies with the transformation temperature, determines the mechanical properties of the steel. Moreover, microindentation testing shows that the microhardness values of UB, LB and martensite are 410~440, 480~550 and 620~640 HV0.1, respectively, further confirming the metallographic observations.

**Table 2**
The heat treatment cycles and the correspondent volume fraction of bainite in B/M microstructure.

| Specimen | | Heat treatment cycle | $V_B$ (vol%) |
|---|---|---|---|
| Q & T | | 1153 K, 1.2 ks→quench→873 K, 3.6 ks→quench | 0 |
| Route 1 | BM1 | 1153 K, 1.2 ks→623 K, 90 s→quench | 50 |
| | BM2 | 1153 K, 1.2 ks→623 K, 120 s→quench | 55 |
| | BM3 | 1153 K, 1.2 ks→623 K, 600 s→quench | 75 |
| Route 2 | BM4 | 1153 K, 1.2 ks→583 K, 600 s→quench | 45 |
| | BM5 | 1153 K, 1.2 ks→583 K, 3.6 ks→quench | 75 |

The isothermal transformation below $M_s$ was performed at 583 K (310 °C). The low transformation temperature depresses the formation of UB. As shown in Fig. 1g-j, representative acicular LB morphology was observed in both specimens. After isothermal transformation below $M_s$ for 3. ks only ~25% of tempered martensite/martensite (TM/M) remains (Fig. 1i-j). However, if the duration of isothermal transformation reduces to 600 s, TM/M dominates (Fig. 1g-h). TEM bright-field micrographs of BM5 depict that fully-transformed grains of prior austenite are divided by the sheaves of LB, lath martensite and TM (Fig. 2a). A microstructural refinement prevails here. The width of lath martensite is comparable width with the sheaves of LB (Fig. 2b). Inside the LB sheaves, a fine dispersion of nanoscale carbides was observed (Fig. 2c-d). These carbides have a lath-shape and are distributed in the acicular ferrite sheaves at a 55~60° angle, with long axes of bainite ferrite (Fig. 2d). The aspect ratio (thickness/length) of such sheaves is relatively small, which can be explained by the low transformation temperature [12]. With further isothermal transformation, LB grew to a limited size by repeated nucleation of subunits in the sheaves [13]. Furthermore, no retained austenite was detected in the TEM dark-field investigations within the dimensional limit of the examinations.

### 3.2. Mechanical properties

In order to investigate the effect of the mixed B/M microstructure on the mechanical properties of the 42CrMo4 steel, tensile testing was conducted. The results are listed in Table 3 in detail. The average errors for the *UTS* and proof stress are ± 15 and ± 20 MPa, respectively. Increasing the duration of conventional austempering at 623 K (350 °C) yields a decrease of $R_{p0.2}$, $A$, $Z$ and $r_1$ simultaneously, especially the parameters for the ductility. Compared to specimen BM1, $A$ and $Z$ of BM3 reduce drastically for 45.1% and 73.5%, presumably due to the increased volume fraction of UB. The *UTS* drops by 16.0% after 30 s further tempering of BM1 and even further tempering barely changes the *UTS*. The proof stress to the *UTS* ratio is held below 0.80, which is desirable for a good fatigue resistance. The mechanical properties of BM4 is comparable with BM1. Its *UTS* is 8.4% lower and $A$ 29.4% higher while $R_{p0.2}$ and $Z$ are quite similar with each other. The specimen BM5 shows the highest *UTS*, $R_{p0.2}$, $A$ and $r_1$ in all of these isothermal transformed samples. $r_1$ amounts to 0.86, which is typical for a high-strength steel. In summary, isothermal transformation below $M_s$ achieves a combination of high strength and high ductility simultaneously. Such a balance between the strength and ductility of 42CrMo4 steel has not been achieved by a conventional Q & T treatment according to DIN EN 10083-3: 2007-01.

### 3.3. Fractography

The fracture surfaces of the tensile specimens after conventional austempering at 623 K (350 °C) are shown in Fig. 3a-d. A clear transition from ductile to cleavage rupture was observed. The specimen BM1 (Fig. 3b) possesses a similar fracture surface as the Q & T specimen (Fig. 3a). The ruptured surface is covered with deep dimples as usually seen in a ductile fracture mode. With further austempering